PENERBIT UMT
Menjana Khazanah Ilmuwan

Journal of Mathematical Sciences and Informatics
Journal Homepage: https://journal.umt.edu.my/index.php/jmsi
eISSN: 2948-3697
DOI: http://doi.org/10.46754/jmsi.2021.12.003

APPROXIMATE ANALYTICAL STUDY OF UNSTEADY FLOW AND HEAT TRANSFER ANALYSIS OF CARBON NANOTUBES NANOFLUID OVER STRETCHING SHEET

ALI REHMAN[1], ZABIDIN SALLEH[1*] AND MUHAMMAD ZEB[2]

[1]Department of Mathematics, Faculty of Ocean Engineering Technology and Informatics, Universiti Malaysia Terengganu, 21030 Kuala Nerus, Terengganu, Malaysia; alirehmanchd8@gmail.com, zabidin@umt.edu.my, [2]Department of Mathematics, COMSATS University Islamabad, Attock Campus; zeb@cuiatk.edu.pk

Corresponding author: zabidin@umt.edu.my

ARTICLE INFO

Article History:
Received June 2021
Accepted September 2021
Available online
December 2021

Keywords:
Nanofluid;
CNTs;
Stretching sheet;
OHAM;
Heat transfer

ABSTRACT

The aim of this paper is to study approximate analytical unsteady flow and heat transfer analysis of CNTs nanofluid over stretching sheet for the improvement of heat assignment ratio. The present work has some important application in industry and engineering because the heat transfer ratio of nanofluid is larger compared to other fluid. With the help of defined similarity transformation, the nonlinear partial differential equations is converted to nonlinear ordinary differential equations. The model of nonlinear ordinary differential equations are then solved by Optimal Homotopy Asymptotic Method. The impact of different parameters are then interpreted using graphs in the form of velocity and temperature profiles. The influence of skin friction coefficient and Nusselt number is presented in the table form.

2020 Mathematics Subject Classification: 65M25, 76W05

INTRODUCTION

Due to its important application in industry, stretching flow is an active area of research in the fluid dynamics. Among the important applications of stretching flow in industry are aerodynamic extrusion of plastic sheet, cooling of metallic plate hot rolling and so on. Sakiadis [1] for the first time introduced stretching flow, they used continuous surface to discuss boundary layer flow. Cran [2] used stretching sheet to find the closed form solution. With the help of this, they showed that the velocity is proportional to the distance from the slit, the researchers [3-9] studied the flow problem over stretching surface. Rehman *et al.* [10] studied analytically the effect of viscous dissipation of thin film time dependent nanofluid by using stretching surface. Common fluids, such as water, oil, and glycol, have too low a heat transfer ratio. To increase the heat transfer ratio, many methods are introduced. With the help of this method, nanofluid is introduced. Nanofluid is a stable suspended solid nanoparticle colloidal solution. The size of the nanoparticle is about 1-100 nm. From the study of nanofluid, it is observed that nanofluid is a little nanoscale division of metal oxide, nitrides, carbides and carbon nanotube (CNT). Ganguly *et al.* [11] investigated the consequence of line dipole and magnetic field for forced convection heat transfer. Malvandi and Ganji [12] investigated the theoretical consequence of magnetic dipole and the effect of nanoparticle moment in a perpendicular conduit. Haghshenas Fard *et al.* [13] used a circular tube to investigate the laminar connective heat transfer of nanofluid. Bahremand *et al.* [14] studied experimentally the turbulent nanofluid flow. Lee *et al.* [15]

used the hot-wire method to discuss nanoliquids comprising oxide nanoparticles and measured their thermal conductivity.

Maciver *et al.* [16] studied the specific models of η and Al_2O_3. Sheikhzadeh *et al.* [17], Wang *et al.* [18], Hamilton and Crosser [19] and Maiga *et al.* [20] investigated the thermo physical properties of nanofluids. Ahmed *et al.* [21] studied analytically the influence of an operative Prandtl model flow of γAl_2O_3-$C_2H_6O_2$ and γAl_2O_3-H_2O nanofluids. Rashidi *et al.* [22] used sheet movements to investigate the influence of the same nanofluid. Hayat *et al.* [23] used the entropy generation to investigate the influence of the same nanofluid. Anderson and Valens [24] gave the idea of magnetic field using magnetic dipole. Zeeshan and Majeed [25] used the spreading surface to explain the influence of magnetic dipole by including Jeffery fluid. Noor and Nadeem [26] used the consequence of magnetic dipole to study nanofluid flow. The most popular class of carbon family is carbon nanotube (CNT). Carbon nanotube is used as a nanomaterial to increase heat transfer. Single wall carbon nanotube (SWCNT) and multi wall carbon nanotube (MWCNT) are two subclasses of carbon nanotube. The main application of carbon nanotube in engineering are for fluidization and heat exchange. Carbon nanotube were introduced by Iijima [27]. In 1991 lijima introduced the multi wall carbon nanotube (MWCNT) using the Krastschmer and Huddman method [27]. Donald Bethune in 1993 also studied MWCNT [28]. They discussed the diameter range of MWCNT and showed that the diameter range of MWCNT is 0.4 x $10^{-9}m$ to 3 x $10^{-9}m$, see also [29]. In MWCNT, there are 2 to 50 coaxial nanotubes with diameter range from 3 x $10^{-9}m$ to 30 x $10^{-9}m$, see [30].

Hone [31] found that the thermal conductivity of MWCNT is 3000 $Wm^{-1}K^{-1}$ and for SWCNT is 6600 $Wm^{-1}K^{-1}$ at room temperature. Haq *et al.* [32] investigated engine based CNT and oil based CNTs. Khan *et al.* [33] used stretching plate to discuss Navier slip boundary condition for CNT. Kamali and Binesh [34] used CNT base nanofluid to discuss the model of power law. Rehman *et al.* [35] studied analytically Marangoni convection of thin film by using stretching cylinder. Inspired by the aforesaid analysis, this paper explains the approximate analytical investigation of unsteady flow and heat transfer of CNTs nanofluid. Mekheimer *et al.* [38] used peristaltic flow to study the effect of the convection flow with the induced magnetic field, heat and mass transfer in the last few years because it has some key applications in several manufacturing processes. Ellahi and Riaz [39] used third grade fluid to discuss the analytical solution for MHD flow. Mukhopadhyay and Gorla [40] used stretching sheet to study unsteady magnetohydrodynamics boundary layer flow. The present work has some important application in industry and engineering because the heat assignment ratio of nanofluid is more compare to other fluid. With the help of defined similarity transformation, the given nonlinear partial differential equation (PDEs) is converted to nonlinear ordinary differential equation (ODEs). The model of nonlinear ordinary differential equations are solved with approximate analytical method. Optimal Homotopy Asymptotic Method (OHAM) is used for the model problem. Liao [36] used this approximate analytical method for the solution of nonlinear differential equation for the first time. The impact of different parameters, are interpreted through graphs in the form of velocity profile and temperature profile. The influence of skin friction coefficient and Nusselt number is presented in the form of tables. The present work is in agreement with published research.

MATHEMATICAL FORMULATION

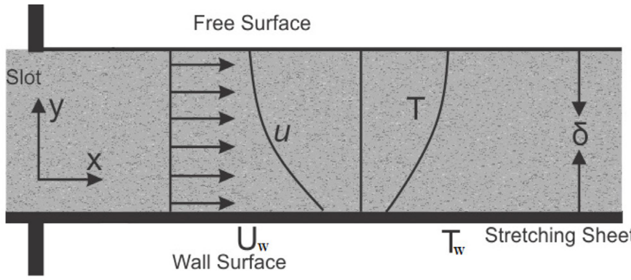

Figure 1: Geometry of the flow problem

Figure 1 shows the geometry of the flow problem. Consider the unsteady compressible laminar flow of CNTs nanofluid for both MWCNT and SWCNT moving over a stretching sheet. Due to the nonlinearity of the stretching sheet, flow is generated by two opposite and equal forces along x-axis. The velocity $U(x,t) = \frac{bx}{1-at}$ of the outer boundary layer is proportional to the point of inertia. $U_w(x,t) = \frac{cx}{1-at}$ is the velocity of the stretching sheet where is a positive constant and is the stretching rate. The continuity, energy and temperature equations are as follows, see [37].

$$\frac{\partial u}{\partial x} + \frac{\partial v}{\partial y} = 0 \tag{1}$$

$$\frac{\partial u}{\partial t} + u\frac{\partial u}{\partial x} + v\frac{\partial u}{\partial y} = \frac{1}{p}\frac{dp}{dx} + v\frac{\partial^2 u}{\partial y^2} - \frac{\sigma B_0^2}{\rho}u \tag{2}$$

$$\frac{\partial T}{\partial t} + u\frac{\partial T}{\partial x} + v\frac{\partial T}{\partial y} = \alpha_m \frac{\partial^2 T}{\partial y^2}\tau\left[D_B\frac{\partial C}{\partial y}\frac{\partial T}{\partial y} + \frac{D_T}{D_\infty}\left(\frac{\partial T}{\partial y}\right)^2\right]. \tag{3}$$

The boundary of the problem is given by

$$u = U_W(x,t), T = T_m \text{ at } y = 0$$
$$u = 0, v = 0, T \to T_\infty \text{ as } y \to \infty \tag{4}$$

Here ρ_{nf} is density of nanofluid and $(C_p)_{nf}$ is specific heat constant, $M = \frac{\sigma B_0^2}{\rho_{nf} c}$ is magnetic parameter, $A = \frac{b}{c}$ R is stretching parameter, R is thermal radiation parameter, $Pr = \frac{v}{\alpha_m}$ is Prandtl number, and S is unsteady parameter, respectively.

With the help of defined similarity transformation, the given nonlinear partial differential equation (PDEs) is converted to nonlinear ordinary differential equation (ODEs) given below

$$\psi = \sqrt{\frac{cv}{1-at}}xf(\eta), \eta = \sqrt{\frac{c}{v(1-at)}}y, \theta = \frac{T-T_m}{T_\infty - T_m} \tag{5}$$

where Ψ is represent stream function and is defined as $u = \frac{\partial\psi}{\partial v}$ and $v = -\frac{\partial\psi}{\partial x}$ which satisfies continuity equation by using this definition

$$u = \frac{cx}{1-at}f'(\eta), v = \sqrt{\frac{cv}{1-at}}f(\eta). \tag{6}$$

Put Eq. (5) and Eq. (6) into Eq. (2) and Eq. (3), the following nonlinear ordinary differential equation is obtained

$$f''' + (1-\phi)^{2.5}\left(1-\phi+\phi\frac{(\rho_s)_{CNT}}{(\rho_f)_{CNT}}\right)\left[ff'' - (f')^2 - \frac{S}{2}\left(f' + \frac{\eta}{2}f''\right)\right] + A^2 - M(1-\phi)^{2.5}(f' - A) = 0 \tag{7}$$

$$\frac{k_{nf}}{k_f}\theta'' PrR\left[1-\phi+\phi\frac{(\rho C_p)_{CNT}}{(\rho C_p)_{CNT}}\right]\left[f\theta' - \frac{S}{2}(\eta\theta')\right] = 0 \tag{8}$$

The boundary condition is given by

$$f'(\eta) = 1, Prf(\eta) + M\theta'(\eta) = 0, \theta(\eta) = 0 \ \ at \ \ \eta = 0$$
$$f'(\eta) = A, \theta(\eta) = 1 \ \ as \ \ \eta \to \infty \tag{9}$$

METHOD OF SOLUTION

The approximate analytical method, namely the Optimal Homotopy Asymptotic Method is used to solve Eq. (7) and Eq. (8) which is given below

$$L(f(\eta)) + N(f(\eta)) + g(\eta) = 0, B(f(\eta)) = 0 \tag{10}$$

where L is linear operator, x is independent variable, $g(\eta)$ is unknown function, N is nonlinear operator and $B(f)$ represents the boundary operator. We the help of the method, we construct a family of equations given below

$$H(\phi(\eta), p) = (1-p)[L(\phi(\eta,p)) + g(\eta)] - H(p)[L(\phi(\eta,p)) + g(\eta) + N(\phi(\eta,p))] = 0$$

$$B(\phi(\eta,p)) = 0 \tag{11}$$

In Eq. (11), p represents embedding parameter which lies in [0,1], $H(p)$ is non-zero auxiliary function for $p \neq 0$ and $H(0) = 0$ and $\phi(\eta,p)$ is an unknown function. Using the initial guessed values and auxiliary linear operators from equations (7) and (8)

$$f_0 = \eta^3 - A + e^{-\eta} \tag{12}$$

$$\theta_0 = \eta^2 - 1 + e^{-\eta} \tag{13}$$

which is obtained from the linear operator

$$f''' + ff'' = 0 \ \ and \ \ \theta'' = 0 \tag{14}$$

with constant properties

$$L_f(C_1 + C_2\eta + C_3\eta^2 + C_4\eta^3) = 0 \ and \ L_\theta(C_5 + C_6\eta) = 0, \tag{15}$$

The residuals error is accessible by Liao [36], so the equations (7) and (8) can be written as

$$\varepsilon_m^f = \frac{1}{n+1}\sum_{j=1}^{n} \left[\kappa_f\left(\sum_{j=1}^{n} f(\eta)_{\eta=j\delta\eta}\right)\right], \tag{16}$$

$$\varepsilon_m^\theta = \frac{1}{n+1}\sum_{j=1}^{n} \left[\kappa_\theta\left(\sum_{j=1}^{n} f(\eta)_{\eta=j\delta\eta}\right), \sum_{j=1}^{n} \theta(\eta)_{\eta=j\delta\eta}\right], \tag{17}$$

$$\varepsilon_m^t = \varepsilon_m^f + \varepsilon_m^\theta. \tag{18}$$

RESULTS AND DISCUSSIONS

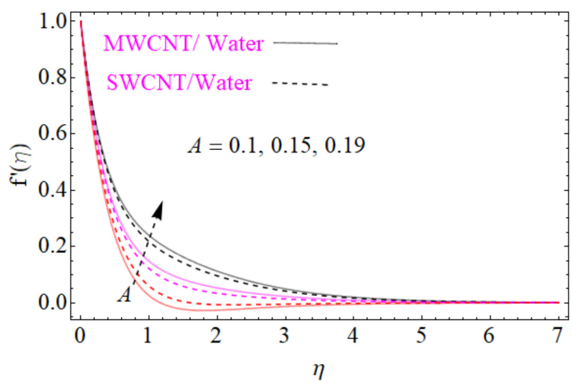

Figure 2: Effect of stretching parameter *A* on the velocity distribution

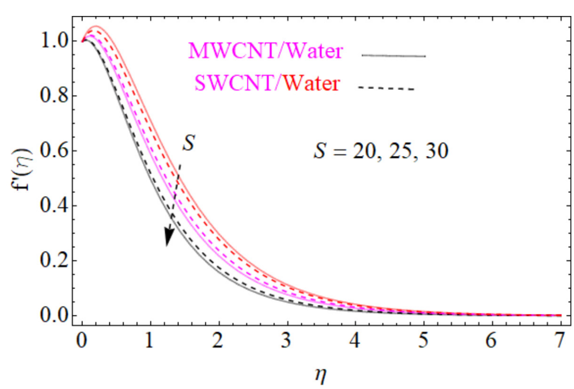

Figure 3: Effect of unsteady parameter *S* against the velocity distribution

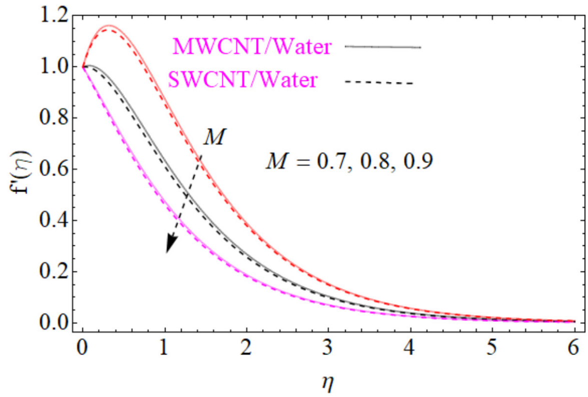

Figure 4: Effect of magnetic field *M* against the velocity distribution

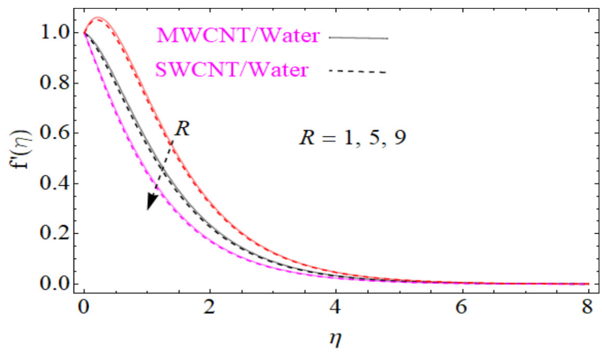

Figure 5: Consequence of thermal radiation parameter *R* against the velocity distribution

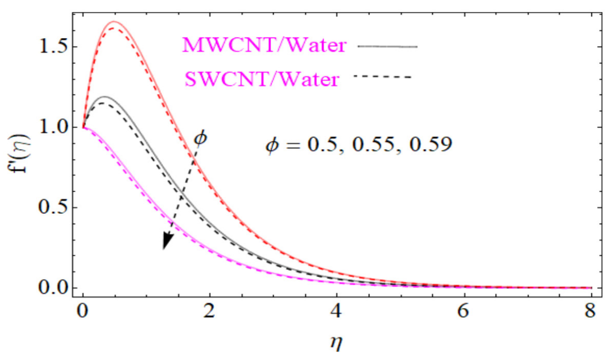

Figure 6: The impress of nanoparticles volume fraction ϕ on the velocity distribution

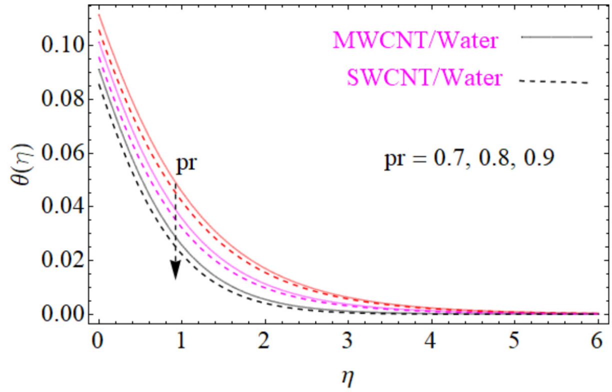

Figure 7: Impress of the Prandtl number *Pr* on temperature distribution

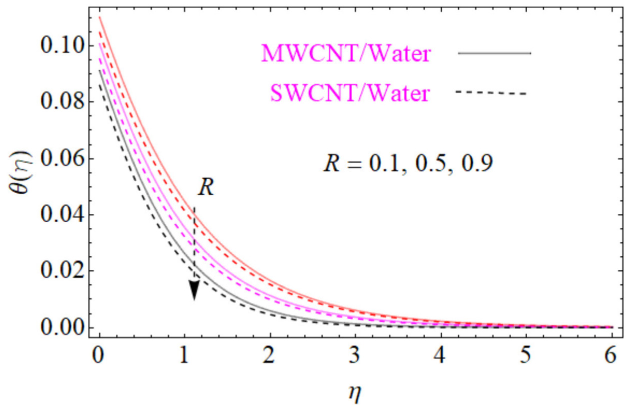

Figure 8: Impression of the thermal radiation parameter *R* against temperature distribution

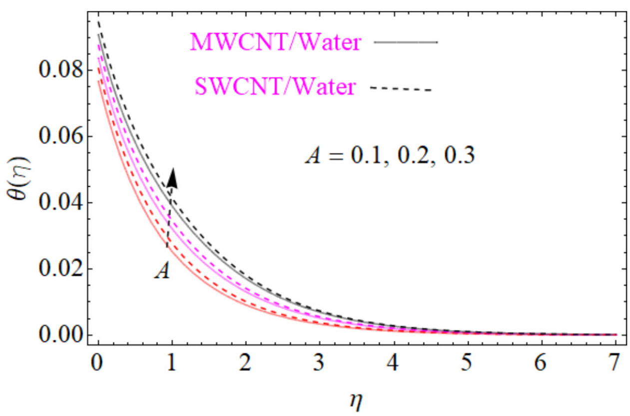

Figure 9: Influence of the stretching parameter on temperature distribution

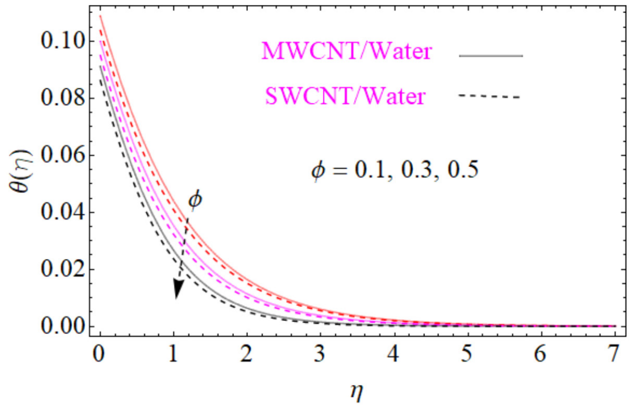

Figure 10: Influence of ϕ on temperature distribution

Table 1: Effect of skin friction for MWCNT and SWCNT when $Pr = 5.6$, $R = 0.1$, $A = 1$

ϕ	M	MWCNT	SWCNT
0.01	0.1	0.5297	0.4947
0.03		0.5416	0.5794
0.05		0.5811	0.5926
	0.2	0.7100	0.6699
	0.3	0.8760	0.9372
		0.9684	0.9546
		0.9981	0.9764

Table 2: Influence of the Nusselt number for the two nanofluids when $\phi = 0.1$, $M = 0.2$, $A = 1$

Pr	R	MWCNT	SWCNT
5.6	1	0.81231	0.89077
6.6		0.79341	0.88237
7.6		0.77451	0.87397
	2	0.75614	0.85647
	3	0.73776	0.84897
		0.72795	0.83121
		0.65021	0.81346

Table 3: The convergence control parameter for SWCNT when $Pr = 6.7$, $M = 0.1$, $R = 0.1$, $\phi = 0.01$, $A = 1$

m	ε_m^f SWCNT	ε_m^θ SWCNT
5	1.36438×10^{-1}	2.86775×10^{-1}
10	7.14094×10^{-3}	1.48738×10^{-2}
15	5.209443×10^{-7}	1.07298×10^{-4}
20	4.37298×10^{-9}	8.54131×10^{-5}
25	3.95787×10^{-11}	7.94423×10^{-6}

Table 4: The convergence control parameter for MWCNT when $Pr = 6.7$. $M = 0.1$, $R = 0.1$, $\phi = 0.01$, $A = 1$

m	ε_m^f MWCNT	ε_m^θ MWCNT
5	1.07991×10^{-1}	2.88574×10^{-1}
10	5.65266×10^{-2}	1.0759×10^{-3}
15	4.12383×10^{-3}	1.0759×10^{-5}
20	3.4616×10^{-4}	8.55721×10^{-7}
25	3.133×10^{-5}	8.006632×10^{-9}

Table 5: OHAM and numerical comparison for $f = (\eta)$

m	**OHAM**	**Numerical**	**Absolute Error**
1	1.00…	1.00…	7.0372×10^{-12}
2	1.03…	1.02…	3.4300×10^{-7}
3	1.05…	1.04…	3.2767×10^{-9}
4	1.06…	1.05…	1.8614×10^{-7}
5	0.99…	0.97…	1.7344×10^{-8}
6	0.89…	0.85…	1.6300×10^{-8}
7	0.76…	0.74…	1.7021×10^{-7}
8	0.61…	0.57…	1.2500×10^{-7}
9	0.42…	0.41…	2.1768×10^{-9}
10	0.22…	0.20…	2.3304×10^{-7}

Table 6: OHAM and numerical comparison for θ (η)

η	**OHAM**	**Numerical**	**Absolute Error**
1	1.00…	1.00…	1.1102×10^{-16}
2	1.31…	1.30…	0.0090
3	1.23…	1.19….	0.0018
4	1.72…	1.70…	0.0250
5	1.82…	1.80…	0.0308
6	1.40…	1.20…	0.0352
7	1.50…	1.30…	0.0384
8	1.22…	1.13…	0.0404
9	1.05…	1.01…	0.0416
10	1.29…	1.11…	0.0421

This section explains the influence of different parameters, like ϕ,M,A,Pr,R,S (nanoparticle volume fraction, stretching parameter, magnetic field parameter, Prandtl number, thermal radiation parameter, and time dependent parameter for both velocity and temperature distribution in graphical from). The effect of different parameter on velocity and temperature distribution is presented from Figures 1-10, Figures 2-6 show the influence of different parameters on velocity distribution and Figures 7-10 show the influence of different parameters on temperature distribution. The impact of skin friction coefficient, Nusselt number and convergence for both velocity and temperature distribution of the given approximate analytical method is presented in Tables 1-4. Table 1 shows the influence of dissimilar parameter on Skin friction. From Table 1 we observe that the skin friction coefficient is the increasing function of nanoparticle volume fraction and magnetic field parameter in both SWCNT and MWCNT. Table 2 shows the influence of different parameter on Nusselt number. From Table 2 we observe the influence of Prandtl number and thermal radiation parameter on Nusselt number, and we see that the relation between Nusselt number, Prandtl number and thermal radiation parameter is inverse in both SWCNT and MWCNT. Tables 3 and Table 4 show the convergence control parameter for the given problem. From Table 3 and Table 4 we see that as we increase the number of iterations, the residual error is decreasing and solid convergence is attained in both SWCNT and MWCNT. The influence stretching parameter A on velocity distribution is presented in Figure 2. We see from Figure 2 that the relation between velocity distribution and stretching parameter is directly related, where velocity distribution increases by increasing velocity distribution parameter as shown in Figure 2. This effect is due to the position of the fluid particle change. As a result, moment of particles rise, so the velocity field is enhanced by the growing value of stretching parameter A. The influence of time dependent parameter S is plotted in Figure 3. From Figure 3 we see that velocity distribution is declining as a function of time dependent parameter as the increasing value of unsteady parameter decreases the velocity field. The impact of magnetic field parameter on velocity distribution is presented in Figure 4. From Figure 4, we see that the relation between velocity distribution and magnetic field parameter is inverse, where the large value of magnetic field parameter decreases the velocity field as shown in Figure 4. This effect is due to the increasing magnetic field M, resistance forces is produced, which opposes the motion of fluid particle which then decreases the velocity distribution. The influence of thermal radiation parameter is presented in Figure 5. From Figure 5 we see that the relation between velocity distribution and thermal radiation parameter is inverse, where the greater value of thermal radiation parameter decreases the velocity distribution. By enhancing the thermal radiation parameter R, resistance forces are produced, which decreases the moment of the fluid particle, so as a result velocity distribution is decreasing. The influence of nanoparticles volume fraction on velocity distribution is presented in Figure 6. From Figure 6 we see that the relation between velocity distribution and nanoparticles volume fraction is inverse, where increasing nanoparticles volume fraction decreases the velocity distribution.

The impact of Prandtl number on temperature distribution is presented in Figure 7. From Figure 7 we see that the relation between temperature distribution and Prandtl number is inverse, where the large value of Prandtl number decreases the temperature distribution. The influence of thermal radiation parameter R on temperature distribution is presented in Figure 8. From Figure 8 we see that the relation between temperature distribution and thermal radiation parameter is opposite. Where enhancing the value of thermal radiation parameter decreases the temperature distribution. The impact of stretching parameter on temperature distribution is presented in Figure 9. From Figure 9 we see that the relation between temperature distribution and stretching parameter is linear, where enhancing the value of the stretching parameter, increases the temperature profile. By growing the stretching parameter A, moment of the fluid particle increases and crash with each other. As a result, the temperature field increases. The impact of nanoparticles volume fraction on temperature field is presented in Figure 10. From Figure 10 we see that the relation between temperature distribution and nanoparticles volume fraction is inverse. That is temperature distribution decreases as the value of the nanoparticles volume increases.

CONCLUSION

The approximate analytical study of CNTs nanofluid for both MWCNT and SWCNT and heat transfer analysis over a stretching sheet has been explained in this research paper. With the help of defined similarity transformation, the given nonlinear partial differential equation (PDEs) is converted to nonlinear ordinary differential equation (ODEs). The model of nonlinear ordinary differential equations are solved with approximate analytical. Optimal Homotopy Asymptotic Method (OHAM) is used for the model problem. Liao [36] used this approximate analytical method for the first time. The impact of different parameters, are interpreted through graphs in the form of velocity distribution and temperature distribution. The influence of skin friction coefficient and Nusselt number is presented in the form of tables. The present research is in agreement with published work. The attained results are deliberated as follows:

- The greater value of nanoparticles volume fraction ϕ, declines the velocity distribution.
- The large value of stretching parameter A, increases the velocity distribution .
- The large value of thermal tradition parameter R, decreases the velocity distribution.
- The large value of Prandtl number Pr, decreases the temperature distribution.
- The large value of stretching parameter A, increases the temperature distribution.
- The large value of magnetic field M, decreases the velocity distribution.

NOMENCLATURE

Stretching parameter	A
Unsteadiness parameter	S
Density of the nanofluids	ρ_{nf}
Thermal radiation parameter	R
Heat generation/absorption parameter	Q
Local Temperature	T
Magnetic field	M
Nusselt number parameter	Nu
Prandtl number parameter	Pr
Specific heat of the nanofluid	C_p
Stretching velocity of the sheet	W_w
Similarity variable	η
Skin friction	C_f
Solid particle volume fraction	φ
Thickness of the liquid film	δ
Temperature at the free surface	T_δ
Thermal conductivity of the nanoparticle's	k_{nf}
Velocity components	(u,w)

CONFLICTS OF INTEREST

The authors declare that there is no conflict of interest. The funders had no role in the design of the study; in the collection, analyses, or interpretation of data; in the writing of the manuscript, or in the decision to publish the results.

ACKNOWLEDGEMENTS

This research has been partially supported by Universiti Malaysia Terengganu under the Postgraduate Research Grant (PGRG) vote no. 55193/3.

REFERENCES

[1] B. C. Sakiadis. (1961). Boundary layer behavior on continuous solid surfaces: I Boundary layer equations for two dimensional and axisymmetric flow, II. Boundary layer on a continuous flat surface. *AICHE J.*, *7*, 221-225.

[2] L. J. Crane. (1970). Flow past a stretching plate. *ZAMP*, *21*, 645-647**.**

[3] P. S. Gupta & A. S. Gupta. (1977). Heat and mass transfer on a stretching sheet with suction or blowing. *Can. J. Chem. Eng.*, *55*, 744-746.

[4] K. G. Kumar, B. J. Gireesha, S. Manjunatha & N. G. Rudraswamy. (2017). Effect of nonlinear thermal radiation on double-diffusive mixed convection boundary layer flow of viscoelastic nanofluid over a stretching sheet. *Int. J. of Mech. and Mat. Eng.*, *12*(1), 18.

[5] K. G. Kumar, B. J. Gireesha, N. G. Rudraswamy & S. Manjunatha. (2017). Radiative heat transfers of Carreau fluid flow over a stretching sheet with fluid particle suspension and temperature jump. *Results in Physics*, *7*, 3976-3983.

[6] K. G. Kumar, B. J. Gireesha & R. S. R. Gorla. (2018). Flow and heat transfer of dusty hyperbolic tangent fluid over a stretching sheet in the presence of thermal radiation and magnetic field. *Int. J. Mech. and Mat. Eng.*, *13*(1), 1-11.

[7] K. G. Kumar, B. J. Gireesha, G. K. Ramesh & N. G. Rudraswamy. (2018). Double-diffusive free convective flow of Maxwell nanofluid past a stretching sheet with nonlinear thermal radiation. *Journal of Nanofluids*, *7*(3), 499-508.

[8] M. R. Krishnamurthy, K. G. Kumar, B. J. Gireesha & N. G. Rudraswamy. (2018). MHD flow and heat transfer (PST and PHF) of dusty fluid suspended with alumina nanoparticles over a stretching sheet embedded in a porous medium under the influence of thermal radiation. *Journal of Nanofluids*, *7*(3), 527-535.

[9] K. G. Kumar, N. G. Rudraswamy, B. J. Gireesha & S. Manjunatha. (2017). Non-linear thermal radiation effect on Williamson fluid with particle-liquid suspension past a stretching surface. *Results in Physics*, *7*, 3196-3202.

[10] A. Rehman, T. Gul, Z. Salleh, S. Mukhtar, F. Hussain, K. S. Nisar, & P. Kumam. (2019). Effect of the Marangoni convection in the unsteady thin film spray of CNT nanofluids. *Processes*, *7*(6), 392.

[11] R. Ganguly, S. Sen & I. K. Puri. (2004). Heat transfer augmentation using a magnetic fluid under the influence of a line dipole. *J. Magn. Magn. Mater*, *271*, 63-73.

[12] A. Malvandi & D. D. Ganji. (2015). Effects of nanoparticle migration on hydromagnetic mixed convection of alumina/water nanofluid in vertical channels with asymmetric heating. *Phys E.*, *66*, 181-196.

[13] M. Haghshenas Fard, M. N. Esfahany & M. R. Talaie. (2010). Numerical study of convective heat transfer of nanofluids in a circular tube two-phase model versus single-phase model. *Int. Communic. Heat Mass Transf.*, *37*, 91-97.

[14] H. Bahremand, A. Abbassi, M. Saffar-Avval. (2015). Experimental and numerical investigation of turbulent nanofluid flow in helically coiled tubes under constant wall heat flux using Eulerian–Lagrangian approach. *Powder Technol.*, *269*, 93-100.

[15] S. Lee, S. U. S. Choi, S. Li & J. A. Eastman. (1992). Measuring thermal conductivity of fluids containing oxide nanoparticles. *Journal of Heat Transfer*, *121*, 280-289.

[16] D. S. Maciver, H. H. Tobin & R. T. Barth. (1963). Catalytic aluminas I. Surface chemistry of eta and gamma alumina. *J. Catal*., *2*, 487–497.

[17] G. A. Sheikhzadeh, M. M. Fakha & H. Khorasanizadeh. (2017). Experimental investigation of laminar convection heat transfer of Al_2O_3-Ethylene Glycol-Water

nanofluid as a coolant in a car radiator. *Journal of Applied Fluid Mechanics*, *10*, 209-219.

[18] X. Wang, X. Xu & S. U. S. Choi. (1999). Thermal conductivity of nanoparticles-fluid mixture. *Journal of Thermo-physics and Heat Transfer*, *13*, 474-480.

[19] R. L. Hamilton & O. K. Crosser. (1962). Thermal conductivity of heterogeneous two component systems. *Industrial and Engineering Chemistry Fundamentals*, *1*, 187-191.

[20] S. E. B. Maiga, C. T. Nguyen, N. Galanis & G. Roy. (2004). Heat transfer behaviors of nanofluids in a uniformly heated tube. *Super Lattices and Microstructures*, *35*, 543-55.

[21] N. Ahmed, Adnan, U. Khan & S. T. Mohyud-Din. (2017). Influence of an effective Prandtl number model on squeezed flow of γAl_2O_3-$C_2H_6O_2$ and γAl_2O_3-H_2O nanofluids. *Journal of Molecular Liquids*, *238*, 447-454.

[22] M. M. Rashidi, V. N. Ganesh, H. A. K. Abdul, B. Ganga & G. Lorenzini. (2016). Influences of an effective Prandtl number model on nanoboundary layer flow of Al_2O_3-H_2O and γAl_2O_3-$C_2H_6O_2$ over a vertical stretching sheet. *International Journal of Heat and Mass Transfer*, *98*, 616-623.

[23] T. Hayat, F. Shah, M. Ijaz Khan, M. Imran Khan & A. Alsaedi. (2018). Entropy analysis for comparative study of effective Prandtl number and without effective Prandtl number via γAl_2O_3-H_2O and γAl_2O_3-$C_2H_6O_2$ nanoparticles. *J. Molecular Liquids*, doi:10.1016/j.molliq.2018.06.029.

[24] H. I. Andersson & O. A. Valnes. (1998). Flow of heated ferrofluid over a stretching sheet in the presence of a magnetic dipole. *Acta Mech*., *128*, 39-47.

[25] A. Zeeshan, A. Majeed & R. Ellahi. (2016). Effect of magnetic dipole on viscous ferro-fluid past a stretching surface with thermal radiation. *J. Molecular Liquids*, *215*, 549-554.

[26] M. Noor & S. Nadeem. (2017). Ferrite nanoparticles Ni-$ZnFe_2O_4$, Mn-$ZnFe_2O_4$ and Fe_2O_4 in the flow of ferromagnetic nanofluid. *Eur. Phys. J. Plus*, *132*, 377.

[27] S. Iijima. (1991). Helical microtubules of graphitic carbon. *Nature*, *354*, 56-58.

[28] P. M. Ajayan & S. Iijima. (1993). Capillarity-induced filling of carbon nanotubes. *Nature*, *361*, 333-334.

[29] C. W. S. To. (2006). Bending and shear moduli of single–walled carbon nanotubes. *Finite Elem. Anal. Des.*, *42*(5), 404-413.

[30] M. S. Dresselhaus, G. Dresselhaus & R. Saito. (1995). Physics of carbon nanotubes. *Carbon*, *33*(7), 883-891.

[31] J. Hone. (2004). Carbon nanotubes: Thermal properties. *Dekker Encycl Nanosci. Nanotechnol*., *7*, 603-610.

[32] R. U. Haq, S. Nadeem, Z. H. Khan & N. F. M. Noor. (2015). Convective heat transfer in MHD slip flow over a stretching surface in the presence of carbon nanotubes. *Phys. B Condens. Matter*, *457*, 40-47.

[33] W. A. Khan, Z. H. Khan & M. Rahi. (2014). Fluid flow and heat transfer of carbon nanotubes along a flat plate with Navier slip boundary. *Appl. Nano Sci*., *4*, 633-641.

[34] R. Kamali & A. R. Binesh. (2010). Numerical investigation of heat transfer enhancement using carbon nanotube-based non-Newtonian nanofluids. *Int. Commun. Heat and Mass Trans*., *37*, 1153-1157.

[35] A. Rehman, Z. Salleh, T. Gul & Z. Zaheer. (2019). The impact of viscous dissipation on the thin film unsteady flow of GO-EG/GO-W nanofluids. *Mathematics*, *7*(7), 653.

[36] S. J. Liao. (2010). An optimal homotopy-analysis approach for strongly nonlinear differential equations. *Communications in Nonlinear Science and Numerical Simulation*, *15*, 2003-2016.

[37] K. G. Kumar, B. J. Gireesha, N. G. Rudraswamy, & M. R. Krishnamurthy. (2019). An unsteady flow and melting heat transfer of a nanofluid over a stretching sheet embedded in a porous medium. *International Journal of Applied Mechanics and Engineering*, *24*(2), 245-258.

[38] Kh. S. Mekheimer. (2008). Effect of the induced magnetic field on peristaltic flow of a couple stress fluid. Phys. Lett. A, 372(23), 4271-4278.

[39] R. Ellahi & A. Riaz. (2010). Analytical solutions for MHD flow in a third-grade fluid with variable viscosity. *Math. Comput. Modelling*, *52*, 1783-1793. https://doi.org/10.1016/j.mcm.2010.07.005

[40] S. Mukhopadhyay & R. S. R. Gorla. (2012). Unsteady MHD boundary layer flow of an upper convected Maxwell fluid past a stretching sheet with first order constructive/destructive chemical reaction. *J. Naval Archit. Mar. Eng.*, *9*, 123-133.